Available online at www.sciencedirect.com
SCIENCE DIRECT
ELSEVIER
International Journal of Thermal Sciences 43 (2004) 915–921
International Journal of Thermal Sciences
www.elsevier.com/locate/ijts

Analysis of a vapour ejector refrigeration system with environment friendly refrigerants

A. Selvaraju, A. Mani *

Refrigeration and Air-conditioning Laboratory, Department of Mechanical Engineering, Indian Institute of Technology Madras, Chennai 600 036, India

Received 10 September 2003; accepted 15 December 2003

Available online 17 April 2004

Abstract

Vapour ejector refrigeration system yields better performance when the ejector operates at choking-mode. A computer code based on existing one dimensional ejector theory has been developed to carry out a study on performance of the system. When operating conditions are changed, the critical performance parameters of the system get shifted to different critical values. The code includes effects of change in specific heat of the working fluid and friction at the constant-area mixing chamber besides internal irreversibility of the ejector. The simulated performance results are compared with the available experimental data from the literature for validation. The effects of operational parameters and ejector configurations of the system on critical performance are studied. Also, comparison of performance of the system with environment friendly refrigerants, R134a, R152a, R290, R600a and R717 is made.

Keywords: Solar energy; Refrigeration; Ejector; Eco-friendly refrigerants

1. Introduction

Compression refrigeration system consumes large amount of high-grade energy. Hence, greater emphasis was made to replace the above system with heat-operated systems that can use abundantly available low-grade energy as the main driving source. Among the heat-operated systems, the absorption refrigeration system requires relatively high temperature heat source. On the other hand, the ejector refrigeration system is found attractive because it requires relatively low temperature heat source. Though steam-ejector refrigeration system became popular as the first type of ejector refrigeration system, the need for higher intensity heat source above 150 °C made it disadvantageous when compared with the vapour-ejector refrigeration system (VERS), which could be operated satisfactorily at generator temperature as low as 65 °C with suitable refrigerants. The temperature of this magnitude can easily be achieved by harnessing solar energy with a flat plate collector or any other source like geothermal energy, waste heat, etc.

Ozone depletion and possible global warming by halogenated chlorofluorocarbons have become international issues due to the potential harm to the environment. In accordance with the Montreal and subsequent Protocols on substances that deplete the ozone layer, CFCs and HCFCs are subjected to total phase-out in a scheduled time-frame. With the above fact in mind, environment friendly refrigerants are considered for the analysis of the system in the present study.

The ejector is the vital component of the VER system. Design of an ejector and evaluation of its operational characteristics have become the core topics of interest for research in recent years. With an aim to predict the satisfactory performance of the ejector, theories on the basis of fluid dynamics were proposed in the middle of the last century. Keenan et al. [1] developed a 1-D ejector theory based on gas dynamics with ideal gas as a working fluid. Heat and friction losses were not considered for the analysis. Defrate et al. [2] proposed a computer code for the evaluation of performance of an ejector system working with ideal gases using the above theory. With a new ejector theory, Munday et al. [3] postulated that primary stream does not mix with entrained stream until the onset of secondary choking at a hypothetical throat in the converging section. After mixing, the mixed stream starts with a supersonic velocity at a uniform pressure

* Corresponding author.
E-mail address: mania@iitm.ac.in (A. Mani).

1290-0729/$ – see front matter © 2004 Elsevier SAS. All rights reserved.
doi:10.1016/j.ijthermalsci.2003.12.005

Nomenclature

A	area	m^2
d	diameter	m
f	friction factor	
h	specific enthalpy	$kJ \cdot kg^{-1} \cdot K^{-1}$
l	length	m
m	mass flow rate	$kg \cdot s^{-1}$
P	pressure	kPa
T	temperature	K
v	specific volume	$m^3 \cdot kg^{-1}$
V	velocity	$m \cdot s^{-1}$

Greek symbols

η	efficiency
μ	critical entrainment ratio, $= m_s/m_p$
ξ	driving pressure ratio (P_g/P_c)

Subscripts

as	after shock
c	condenser
d	diffuser
$d1$	diffuser inlet
$d2$	diffuser outlet
e	evaporator
g	generator
is	isentropic
m	mixing chamber
opt	optimum
p	primary fluid
pe	primary fluid exit
t	throat
s	secondary fluid
sc	secondary flow choking
se	secondary fluid exit

Abbreviation

CFC	chlorofluorocarbon
COP	coefficient of performance
CR	compression ratio, $= P_c/P_e$
HCFC	hydrochlorofluorocarbon
VER	vapour ejector refrigeration

till it experiences a normal shock at the constant area cross-section and further decelerates to condenser pressure in the diffuser. Eames et al. [4] carried out an analytical study for predicting the performance of the VER system with steam as working fluid. With a computer simulation model, Sun et al. [5] examined the performance of a ejector refrigeration system with HCFC-123 as working fluid. They included a regenerator and a pre-cooler for improving the system performance. Huang et al. [6–8] carried out a 1-D analysis for the prediction of the ejector performance with an assumption that hypothetical throat occurs inside the cylindrical chamber and mixing occurs in this constant-area mixing chamber at a fairly uniform pressure. Since the assumption of ideal gas for analysis could bring significant error, Zeren et al. [9] described mathematically an ejector cooling system with R12 as refrigerant and solar energy as the driving source. They have directly introduced thermodynamic properties of the working fluid for the analysis. With the analytical review of experimental study, Paliwoda [10] has illustrated that halocarbon vapour jet refrigeration systems are suitably preferred when low-grade heat and ample condenser cooling facilities are available. It is further concluded that though superheating of primary jet results in a considerable increase in entrainment ratio and system efficiency, it does not bring any cost benefit. With the thermodynamic analysis of the cycle and making use of an empirical correlation obtained from experimentation, Dorantes et al. [11] predicted the performance of a jet cooling system operating with pure refrigerants and non-azeotropic mixtures. They have concluded that the entrainment ratio and the system efficiency depend mainly on the nature of the working fluid. In the same line by developing a simulation program, Bourmaraf et al. [12] have investigated and compared the performance of a jet cooling system using zeotropic and azeotropic refrigerant mixtures as substitutes of pure refrigerants. Cizungu et al. [13] developed a computer code and analyzed the performance of an ejector refrigeration system operating with pure refrigerants that are environment friendly. Research works on VERS with ejectors having fixed geometrical parameters are found in many literatures [6–8,10,13,14]. The ejector with fixed geometrical dimensions gives a better performance with higher entrainment ratio, when it is operated at choking-mode [5]. To obtain this better performance at different operating conditions, area ratio of the ejector is varied. A computer code has been written to analyze performance of the ejector at critical mode. The code includes effect of friction at the constant-area mixing chamber and effect of change in specific heat of the working fluid besides internal irreversibility of the ejector. In this paper, the effect of operational parameters on performance of the system with environment friendly refrigerants like, R134a, R152a, R290, R600a and R717 is presented. Validation of simulated performance results is carried out with the available experimental data from the literatures. The performance is evaluated within the range of generator temperature that can easily be achieved by harnessing solar energy with a flat plate collector.

2. Description of the system

Schematic diagram of the VER system selected for analysis is shown in Fig. 1. A descriptive configuration of the

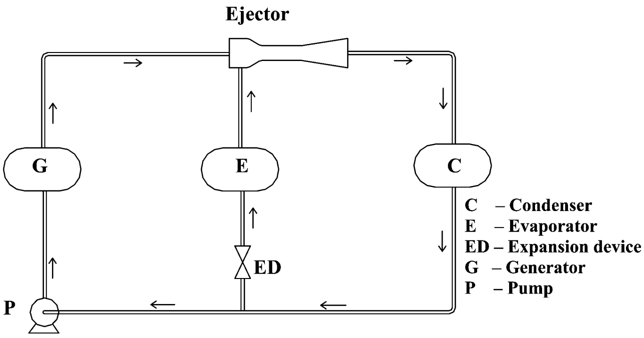

Fig. 1. Schematic diagram of vapour ejector refrigeration system.

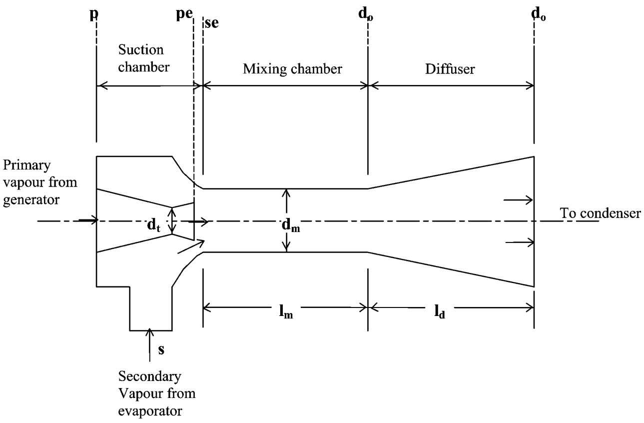

Fig. 2. Schematic diagram of ejector.

ejector is depicted in Fig. 2. The system consists of a generator, ejector, condenser, expansion device and liquid pump. The generator supplies high-pressure vapour by converting liquid due to absorption of heat. This high-pressure vapour is expanded through the convergent–divergent nozzle in the ejector to produce high velocity stream, which entrains the vapourized refrigerant from the evaporator. Both the fluids mix together in the mixing chamber. Pressure raise occurs in the ejector due to formation of shock followed by flow through the diffuser. The pressurized fluid undergoes condensation in the condenser. A portion of the condensate is passed through an expansion device to the evaporator for realizing the refrigeration effect. The remaining liquid is pumped back to the generator through the liquid pump.

3. Analysis of the ejector

Choking of flow is observed at different sections of an ejector. 'Primary flow choking' exists at the throat of the primary convergent–divergent nozzle. 'Secondary flow choking' occurs at the interface between primary and secondary fluid before mixing. These choking phenomena play a vital role in deciding the critical operational parameters of an ejector. 'Mixed fluid choking' is expected to occur in the constant-area mixing chamber. Since flow of mixed fluid is supersonic, formation of a normal shock, that converts the flow to subsonic, is expected before the fluid enters the diffuser. The plane of choking at which Mach number becomes unity is supposed to get merged with that of the shock wave. Thus, in the mixed fluid flow, the phenomenon of shock overtakes the choking predominantly and makes the formulation for analysis of mixed fluid choking insignificant.

When the working fluid passes through ejector, it is subjected to losses of flow due to fluid and wall frictions at different sections. These losses are accounted in terms of efficiencies referred to ideal isentropic transforms. They are generally identified on the basis of the flow passage like nozzle efficiency for primary fluid flow, suction or secondary fluid flow efficiency, mixed fluid flow efficiency and diffuser efficiency. Coefficients of losses for primary fluid flow, secondary fluid flow and mixed fluid flow in the diffuser are not very sensitive to analytical results. But, when mixed fluid passes through cylindrical mixing chamber, it experiences loss due to friction at the wall surface. During the analysis it is observed that the coefficient of friction is a very sensitive factor in deciding the efficiency of mixing and subsequently the exit pressure of the ejector. Since the fluid enters the constant-area mixing chamber at supersonic velocity with high Reynolds number, the friction factor is found out using the following equation with the assumption that the inside surface of the mixing chamber is smooth [16]

$$\frac{1}{\sqrt{f_m}} = 2.0 \log\left(Re_m \sqrt{f_m}\right) - 0.8 \tag{1}$$

The above expression is an equation of straight line, with which the velocity is assumed to vary linearly along the constant area section. Hence the friction factor is computed as an arithmetic mean value between the inlet and exit of this mixing chamber.

The following assumptions are made for the analysis:

(1) The flow inside the ejector is steady and one dimensional;
(2) The coefficients accounting for losses in the primary flow nozzle, the secondary fluid passage and the diffuser are 0.95, 0.95 and 0.85, respectively, [15];
(3) The heat loss from the ejector is negligible;
(4) Normal shock occurs at the end of the constant-area mixing chamber;
(5) Velocities at the inlets of primary and secondary fluids and at the exit of the diffuser are negligible.

Governing equations for analysis of flow through ejector are obtained by using laws of conservation of mass, momentum and energy.

For driving fluid through primary convergent–divergent nozzle, area to mass flow rate at any cross-section is expressed as,

$$\frac{A}{m_p} = \frac{v_p}{\sqrt{2\eta_p(h_b - h)_{\text{is}}}} \tag{2}$$

Primary flow choking occurs at the section (throat) where the area to mass flow rate at given inlet pressure and temperature becomes minimum. By varying enthalpy along the flow path, the minimum area per mass flow rate is evaluated through iterative process. Hence, the area of the throat per mass flow rate is computed as,

$$\frac{A_t}{m_p} = \frac{v_p}{\sqrt{2\eta_p(h_b - h_t)_{\mathrm{is}}}} \tag{3}$$

For secondary flow choking before mixing, the hypothetical area to mass flow rate at given inlet pressure and temperature of the evaporator is found out as,

$$\frac{A}{m_s} = \frac{v_s}{\sqrt{2\eta_s(h_e - h)_{\mathrm{is}}}} \tag{4}$$

Hence, the critical pressure of the secondary fluid at the beginning of the mixing is obtained. It is assumed that the primary fluid and the secondary fluid start mixing at this critical pressure.

Velocity of primary fluid leaving the nozzle is,

$$V_{\mathrm{pe}} = \sqrt{2\eta_p(h_b - h_{\mathrm{pe}})_{\mathrm{is}}} \tag{5}$$

Velocity of the secondary fluid just before meeting primary fluid is,

$$V_{\mathrm{se}} = \sqrt{2\eta_s(h_e - h_{\mathrm{se}})_{\mathrm{is}}} \tag{6}$$

From mass balance, the mass flow rate of mixed fluid is determined as,

$$m_m = m_p + m_s \tag{7}$$

By applying momentum balance between inlet section and section before shock in the mixing chamber, the velocity of the mixed fluid is expressed as,

$$V_m = \frac{(m_p V_{\mathrm{pe}} + m_s V_{\mathrm{se}}) + (P_{\mathrm{se}} - P_m)A_m}{m_m(1 + \frac{f_m}{2}\frac{l_m}{d_m})} \tag{8}$$

By mass balance, area of constant area mixing chamber for unit mass flow rate of mixed fluid flow is rewritten as,

$$\frac{A_m}{m_m} = \frac{v_m}{V_m} \tag{9}$$

The characteristic area ratio for ejector is found out with the help of the following expression as,

$$\frac{A_m}{A_t} = (1 + \mu)\frac{v_m V_t}{v_p V_m} \tag{10}$$

The normal shock is assumed to occur at the mixing chamber. Using mass, momentum and energy balances, the static pressure rise across the shock is given as,

$$P_{\mathrm{as}} - P_m = \frac{V_m}{v_m}(V_m - V_{\mathrm{as}}) \tag{11}$$

Assuming that the pressure after the shock and the pressure at the diffuser inlet are equal and the mixed stream leaves the diffuser at negligible velocity, the velocity of the fluid at diffuser inlet is determined as,

$$V_{d1} = \sqrt{\frac{2(h_{d2} - h_{d1})_{\mathrm{is}}}{\eta_d}} \tag{12}$$

Incorporating the frictional effect, the expression for critical entrainment ratio is obtained from momentum balance between inlet and exit sections of the mixing chamber as,

$$\mu = \frac{V_{\mathrm{pe}} - V_{d1} - \frac{1}{2}V_{d1} f_m (l_m/D_m)}{V_{d1} - V_{\mathrm{se}} + \frac{1}{2}V_{d1} f_m (l_m/D_m)} \tag{13}$$

Critical performance of the cycle excluding the energy imparted by pump is expressed as,

$$COP = \mu\frac{(h_e - h_c)}{(h_b - h_c)} \tag{14}$$

4. Computation methodology

A computer simulation model has been developed on the basis of the one dimensional ejector theory and its control-volume-based analytical equations. The model includes operating parameters, T_g, T_e, T_c, P_g, P_e and P_c as the input for solving the equations described above. Thermodynamic properties of working fluids are obtained with the package REFPROP. The ratio of cylindrical chamber length to diameter is assumed to be 10 [10]. With the inlet pressure, P_g, of the primary fluid, the throat area, A_t of the nozzle is obtained for maximum flow condition corresponding to primary flow choking at the throat. It is assumed that the mixing of primary and secondary fluids starts at a pressure, P_{se}. This pressure is determined with the inlet pressure, P_e from choking of the secondary fluid at a hypothetical throat near the entrance of the mixing chamber. The state of the mixed fluid is checked for supersonic flow condition and the friction factor within the mixing chamber is computed as explained in Section 3. Subsequently, the existence of a normal shock at the end of the constant-area mixing chamber is probed if the flow before the shock is supersonic. Neglecting the velocity at the diffuser exit, the total pressure raise across the shock and diffuser is matched for the exit pressure of the diffuser, P_c by an iterative process wherein the entrainment of secondary fluid is varied and checked for satisfactory results. This computational procedure yields the output of critical entrainment ratio, μ, and critical COP at different operating conditions.

5. Results and discussion

Validation of the computer simulation model is carried out for R11 with entrainment ratio at two different conditions, one at compression ratio, $CR = 2.2$ and another at $CR = 2.3$, by varying the generator temperature. The simulated performance is compared with that of experimental data available in the literature [14]. Fig. 3(a) shows the effect of driving pressure ratio (P_g/P_c) on critical entrainment ratio. For both cases the simulated results agree fairly well with the experimental data and the maximum deviation is found to be 15%. The validation of simulation code is further

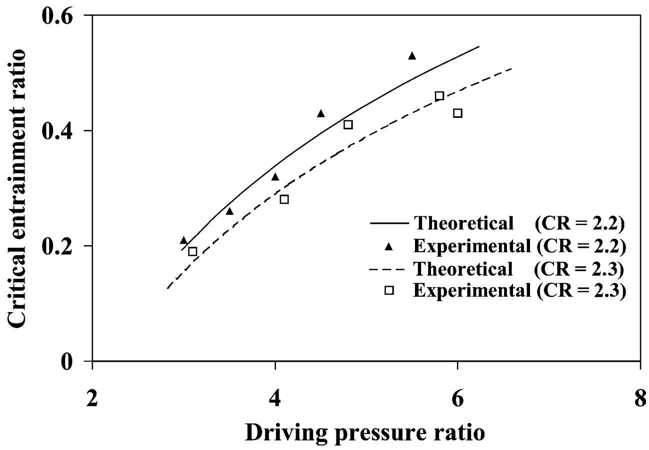

(a)

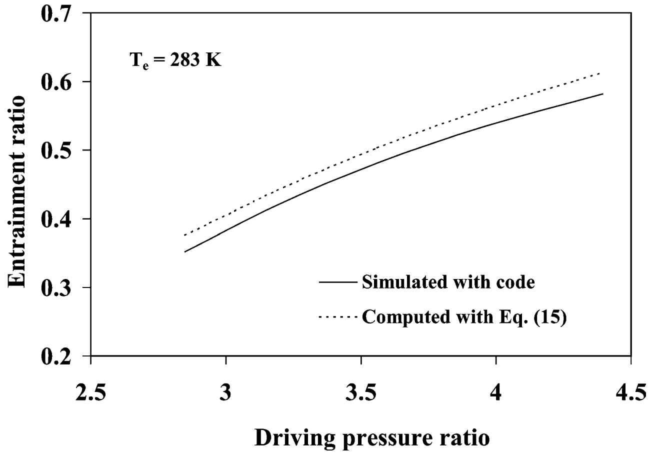

(b)

Fig. 3. (a) Comparison of simulated results for R11 with experimental data [14]. (b) Comparison of the simulated critical entrainment ratio with that from the literatures [11,12].

extended for comparison of the simulated critical entrainment ratio with the critical entrainment ratio described in the literatures [11,12] as,

$$\mu_{\text{opt}} = 3.32\left[\frac{1}{CR}\left(1-\left(\frac{1.21}{\xi}\right)\right)\right]^{2.12} \tag{15}$$

Fig. 3(b) depicts the effect of driving pressure ratio on entrainment ratio in the selected operating range for R134a. The variation of simulated results in this case also is in good agreement with that of data computed using the empirical correlation (15), with a maximum deviation of 7%.

In both of the above cases, the numerical results are interpolated to obtain continuous lines using polynomial functions of the form,

$$y = \sum_{n=0}^{2} b^n x^n$$

where x and y stand for driving pressure ratio and critical entrainment ratio respectively, and b stands for constants that make the uncertainties in fitting continuous lines to be less than 0.01%.

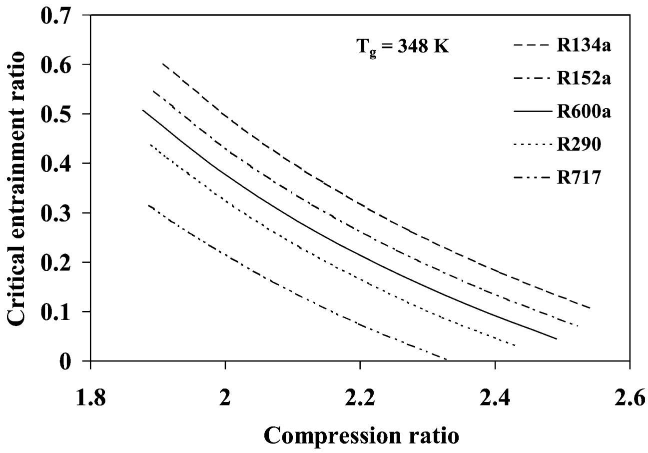

Fig. 4. Effect of compression ratio on critical entrainment ratio.

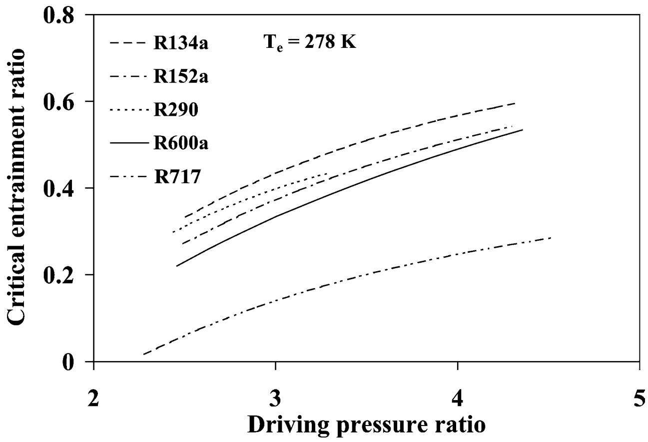

Fig. 5. Effect of driving pressure ratio on critical entrainment ratio.

Fig. 4 shows the effect of compression ratio on critical entrainment ratio obtained for different working fluids. When compression ratio increases at a constant evaporator temperature, the back pressure at the ejector exit increases. Any increase in the back pressure reduces driving pressure ratio and subsequently entrainment ratio. Hence, critical entrainment ratio decreases when compression ratio increases. It can be noticed that critical entrainment ratio of working fluid with higher molecular weight is higher compared to that of fluids with lower molecular weight. Also, the pattern of performance remains same at higher generator temperature. Fig. 5 portrays the variation of critical entrainment ratio with driving pressure ratio at a constant compression ratio. Any increase in driving pressure leads to increase in entrainment from the evaporator. Hence, the critical entrainment ratio increases with increase in the driving pressure ratio. Among the working fluids selected, R134a gives better entrainment ratio at the same operating conditions.

Fig. 6 depicts the variation of critical COP with compression ratio. As stated earlier, the increase in compression ratio at constant evaporator temperature decreases the entrainment from the evaporator. Consequently the refrigerating capacity of the system decreases. Hence COP decreases for

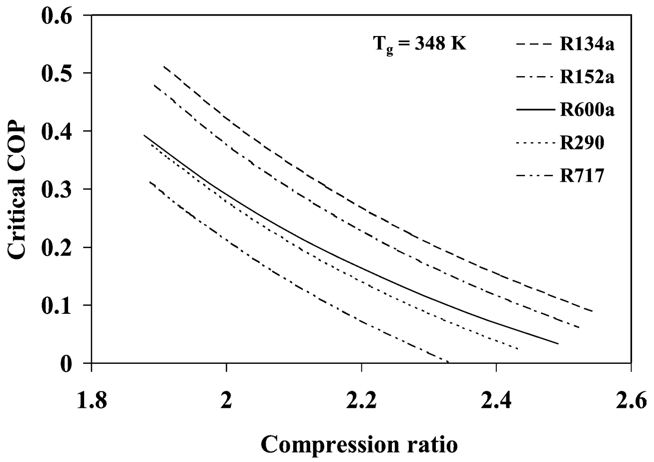

Fig. 6. Effect of compression ratio on critical COP.

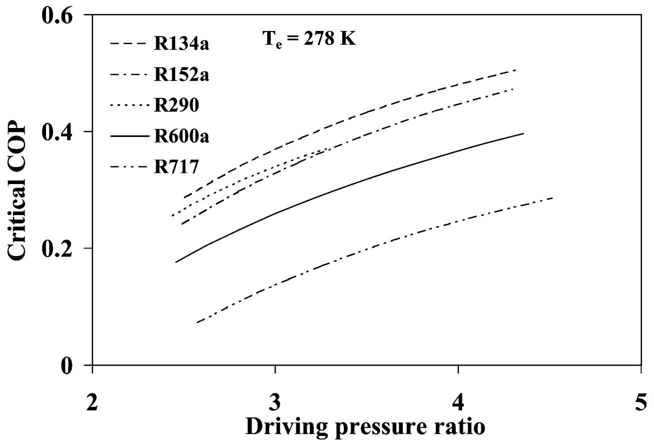

Fig. 7. Effect of driving pressure ratio on critical COP.

all refrigerants as compression ratio increases. Among the working fluids considered, R134a gives better COP in the range considered. Fig. 7 discerns the variation of critical COP with driving pressure ratio. As driving pressure ratio increases entrainment ratio increases resulting in increase of the refrigeration capacity. Hence, the critical COP increases with the increase in driving pressure ratio.

Fig. 8 shows three-dimensional presentation of performance characteristics of the ejector employing R134a as working fluid. It can be noticed that, as explained earlier, the critical entrainment ratio increases with increase in driving pressure ratio and decreases with increase in compression ratio. The same trend of variation is observed for critical COP that increases with increase in driving pressure ratio and decreases with increase in compression ratio as shown in Fig. 9. Pattern of variations for all other selected fluids is found to be similar but at different dimensions in three-dimensional views obtained with the above non-dimensional parameters.

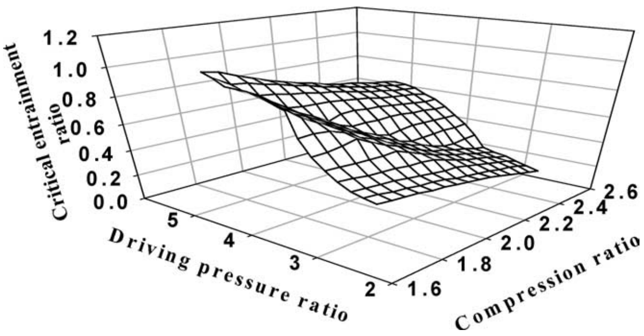

Fig. 8. Variation of critical entrainment ratio with compression ratio and driving pressure ratio.

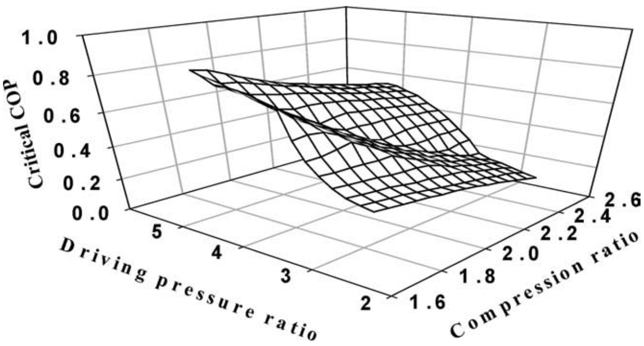

Fig. 9. Variation of critical COP with compression ratio and driving pressure ratio.

6. Conclusions

The influence of compression ratio, and driving pressure ratio on critical entrainment ratio and critical COP of the ejector are studied within the operating range obtainable using a simple solar collector, waste heat etc. As the compression ratio increases the entrainment ratio and COP decreases. As the driving pressure ratio increases the entrainment ratio and COP increases. Among the working fluids considered, the system with R134a gives better performance.

References

[1] J.H. Keenan, E.P. Neumann, F. Lustwerk, An investigation of ejector design by analysis and experiment, in: ASME Annual Meeting, 1949, pp. 299–309.

[2] L.A. Defrate, A.E. Hoerl, Optimum design of ejector using digital computers, Chem. Engrg. Progress Sympos. Ser. 55 (21) (1959) 43–51.

[3] J.T. Munday, D.F. Bagster, A new theory applied to steam jet refrigeration, Industrial Engrg. Chem. Process Des. Dev. 16 (4) (1977) 442–449.

[4] I.W. Eames, S. Aphornratana, H. Haider, A theoretical and experimental study of a small-scale steam jet refrigerator, Internat. J. Refrig. 18 (1995) 378–386.

[5] D.W. Sun, I.W. Eames, Performance characteristics of HCFC-123 ejector refrigeration cycles, Internat. J. Energy Res. 20 (1996) 871–885.

[6] B.J. Huang, J.M. Chang, C.P. Wang, V.A. Petrenko, A 1-D analysis of ejector performance, Internat. J. Refrig. 22 (1999) 354–364.

[7] B.J. Huang, C.B. Jiang, F.L. Hu, Ejector performance characteristics and design analysis of jet refrigeration system, ASME J. Gas Turbines Power 107 (1985) 792–802.
[8] B.J. Huang, J.M. Chang, Empirical correlation for ejector design, Internat. J. Refrig. 22 (1999) 379–388.
[9] F. Zeren, R.E. Holmes, P.E. Jenkins, Design of a Freon jet pump for use in a solar cooling system, in: ASME Winter Annual Meeting, 1978, pp. 1–9.
[10] P. Paliwoda, A review paper on the experimental study on low-grade heat and solar energy operated halocarbon vapour-jet refrigeration systems, Topical studies, IIR Bull. (1968) 1003.
[11] R. Dorantes, A. Lallemand, Prediction of performance of a jet cooling system operating with pure refrigerants or non-azeotropic mixtures, Internat. J. Refrig. 18 (1) (1995) 21–30.
[12] L. Boumaraf, A. Lallemand, Performance of a jet cooling system using refrigerants mixtures, Internat. J. Refrig. 22 (1999) 580–589.
[13] K. Cizungu, A. Mani, M. Groll, Performance comparison of vapour jet refrigeration system with environmentally friendly working fluids, Appl. Thermal Engrg. 21 (2001) 585–595.
[14] E. Nahdi, J.C. Champoussin, G. Hostache, J. Cheron, Optimal geometric parameters of a cooling ejector-compressor, Internat. J. Refrig. 16 (1) (1993) 67–72.
[15] J.J. Henzler, Design of ejectors for single-phase material systems, Ger. Chem. Engng. 6 (1983) 292.
[16] H. Schlichting, Boundar-Layer Theory, McGraw-Hill, New York, 1968.